

MIT Open Access Articles

*Modeling of a Bridge-Shaped Nonlinear
Piezoelectric Energy Harvester*

The MIT Faculty has made this article openly available. *Please share*
how this access benefits you. Your story matters.

Citation: Gafforelli, Giacomo et al., "Modeling of a Bridge-Shaped Nonlinear Piezoelectric Energy Harvester." *Energy Harvesting and Systems* 1, 3-4 (December 2014): 179–187 doi. 10.1515/ehs-2014-0005 ©2014 Authors

As Published: <https://dx.doi.org/10.1515/EHS-2014-0005>

Publisher: Walter de Gruyter GmbH

Persistent URL: <https://hdl.handle.net/1721.1/128843>

Version: Final published version: final published article, as it appeared in a journal, conference proceedings, or other formally published context

Terms of Use: Article is made available in accordance with the publisher's policy and may be subject to US copyright law. Please refer to the publisher's site for terms of use.



Research Article

Giacomo Gafforelli, Ruize Xu, Alberto Corigliano* and Sang-Gook Kim

Modeling of a Bridge-Shaped Nonlinear Piezoelectric Energy Harvester

Abstract: Piezoelectric microelectromechanical systems (MEMS) energy harvesting is an attractive technology for harvesting small energy from ambient vibrations. Increasing the operating frequency bandwidth of such devices is one of the major challenges to be solved for real-world applications. A MEMS-scale doubly clamped nonlinear beam resonator has demonstrated very wide bandwidth and high-power density among the energy harvesters reported. In this paper, a first complete theoretical discussion of nonlinear resonance-based piezoelectric energy harvesting is provided. The sectional behavior of the beam has been studied through the Classical Lamination Theory (CLT) specifically modified to introduce the piezoelectric coupling and nonlinear Green-Lagrange strain tensor. A lumped parameter model has been built through Rayleigh–Ritz method and the resulting nonlinear coupled equations have been solved in the frequency domain through the Harmonic Balance Method (HBM). Finally, the influence of external load resistance on the dynamic behavior has been studied. The theoretical model shows that nonlinear resonant harvesters have much wider power bandwidth than that of linear resonators but their maximum power is still bounded by the mechanical damping as is the case for linear resonating harvesters.

Keywords: MEMS, energy harvesting, piezoelectric material, nonlinear dynamics, classical lamination theory, harmonic balance method

DOI 10.1515/ehs-2014-0005

*Corresponding author: **Alberto Corigliano**, Department of Civil and Environmental Engineering, Politecnico di Milano, Piazza Leonardo da Vinci 32, 20133, Milano, Italy, E-mail: alberto.corigliano@polimi.it

Giacomo Gafforelli, Department of Civil and Environmental Engineering, Politecnico di Milano, Piazza Leonardo da Vinci 32, 20133, Milano, Italy

Ruize Xu, Sang-Gook Kim, Micro and Nano Systems Laboratory, Department of Mechanical Engineering, Massachusetts Institute of Technology, 77 Massachusetts Avenue, Cambridge, MA 02139, USA

Introduction

Piezoelectric microelectromechanical systems (MEMS) have been proven to be an attractive technology for harvesting small amount of energy from ambient vibrations. This technology promises to eliminate the need for replacing chemical batteries or complex wiring in micro-sensors/microsystems, moving us closer toward battery-less autonomous sensor systems and networks. In the meantime, new developments in sensors and complementary metal oxide semiconductor (CMOS) circuitry technology have considerably reduced the power consumption of electronics which can now be powered by a few μW of continuous power from ambient vibrations (Kim, Priya, and Kanno 2012). For MEMS-scale energy harvesters, piezoelectric transduction is the most appropriate scenario since standard MEMS thin-film processes are available for many piezoelectric materials, assuring high efficiency, high energy density and scalability of the device design. Operating frequency, frequency bandwidth, excitation level, power density and size are the key design requirements.

At the present time, most of the devices reported in the literature do not meet the desired requirements mainly due to the very narrow bandwidth and not-low-enough resonant frequency. Cantilever laminated beams with thin films of lead zirconate titanate $\text{Pb}(\text{Zr},\text{Ti})\text{O}_3$ (PZT) on Si or SiN_x have been widely used to achieve high-power generation at large deflections near the resonant frequency (Jeon et al. 2005). However, the frequency bandwidth of the linear resonance system is extremely small, making the harvesters very impractical. Moreover, excessive strain at the exact resonance may shorten the life time of the harvester due to the accelerated piezoelectric fatigue over 0.2% strain on the piezoelectric thin film.

Exploiting nonlinear behaviors has been identified as a possible solution to solve the issues emerged by studying cantilever linear harvesters. The effect of nonlinear piezoelectric constitutive equations has been studied in cantilever beam harvesters showing that one- or two-mode approximations are not sufficient to accurately

predict the performance of the cantilever harvester (Abdelkefi, Nayfeh, and Hajj 2012). Other authors proposed bistable harvesters that exploit instability induced by pre-stresses or additional external magnetic interactions (Harne and Wang 2013). These designs seem promising but still require an external intervention (as glued magnets or pre-stresses) which enhances fabrication-related issues.

A nonlinear resonance-based energy harvester was designed and developed for ultra wide-bandwidth (UWB) energy harvesting (Hajati and Kim 2011). It was demonstrated that both wide enough bandwidth resonance and high enough power density could be achieved by a doubly clamped beam nonlinear resonance energy harvester. A doubly clamped beam at large deflection requires stretching strain in addition to the bending strain to be geometrically compatible, which stiffens the beam as the beam deflects and transforms the dynamics to the nonlinear regime. Interdigitated electrodes were employed to convert the stretching strain into electrical charge through d33-mode piezoelectrics. This device exploits pure geometrical constraints to induce the nonlinear hardening behavior to the clamped beam, in this way it is not required an additional external intervention on the harvester (as for common bistable) and the fabrication complexity is considerably reduced. Moreover, bridge resonant harvesters, in which nonlinear effects are activated due to axial stretching, can easily achieve the full strain capability of the piezoelectric layer since higher longitudinal strains can be obtained at equal transversal displacement with respect to e.g. cantilever linear resonators. This significantly shrinks the size of the device.

In this paper, a first comprehensive theoretical discussion on nonlinear resonance-based piezoelectric energy harvesting is provided. First, the electrical damping is considered as a linear dashpot added to the classical mechanical damper and the influence of the additional damping has been studied. It has been shown that the maximum power generation of nonlinear resonant harvesters is theoretically bounded by the mechanical damping of the dynamic system, which is the same as the well-known result for linear piezoelectric harvesters (duToit, Wardle, and Kim 2005). Theoretical modeling of this damping boundedness is presented here for nonlinear harvesters (Section 2). In Section 3, this result is verified through a more accurate model which considers the influence of an external load resistance to the dynamic behavior of the nonlinear oscillator. The sectional behavior of the doubly clamped beam is studied through the Classical Lamination Theory specifically modified to introduce the piezoelectric coupling and

nonlinear Green-Lagrange strain tensor. A lumped parameters model is built and solved through the Harmonic Balance Method (HBM). The theoretical model shows that nonlinear resonant harvesters have much wider power bandwidth than that of linear resonators, but their maximum power is still bounded by the mechanical damping as is the case for linear resonating harvesters.

Simple model with linear electrical damping

A general nonlinear piezoelectric resonant energy harvester is modeled in Figure 1 by a spring-mass system. k_L and k_N are the linear and nonlinear stiffness, c_M and c_E are the linear mechanical and electrical damping, m_c is the concentrated mass and w is the displacement of the mass relative to the reference system, finally y_{ext} is the displacement of the reference frame to the ground. The system behaves as a Duffing oscillator and its dynamics is described by eq. [1]:

$$m_c \ddot{w} + (c_E + c_M) \dot{w} + k_L w + k_N w^3 = -\ddot{y}_{\text{ext}} m_c \quad [1]$$

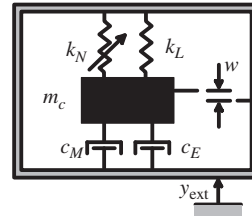


Figure 1 Nonlinear energy harvester with linear electric damping

In the case of a doubly clamped beam, at large deflections the stretching strain increases the stiffness. The hardening behavior is obtained when $k_N > 0$. The solution of eq. [1] is achieved through the HBM in case of harmonic excitation (Worden and Tomlinson 2000). Harmonic balance mimics the spectrum analyzer by simply assuming that the response to a sinusoidal excitation is a sinusoid at the same frequency. A trial solution $w = W \sin(\omega t)$ is substituted in the equation, then the coefficients of the same harmonics are equated and the nonlinear Frequency Response Function (FRF) is computed as shown in eq. [2]:

$$Y = \left\{ \left[-\Omega_M^2 + 1 + \frac{3}{4} \alpha Y^2 \right] + i \left[2(\zeta_E + \zeta_M) \Omega_M \right] \right\}^{-1} \quad [2]$$

where $\alpha = k_N/k_L W_0^2$ is a measure of the nonlinearity of the system, W_0 is the linear static displacement, $Y = W/W_0$ is the dimensionless amplitude, $\Omega_M = \omega/\omega_n$ is the dimensionless excitation frequency, $\zeta_M = c_M/2\omega_n m_c$

and $\zeta_E = c_E/2\omega_n m_c$ are the electrical and mechanical damping ratios.

The equivalent stiffness and the natural frequency are amplitude dependent, which explains the hardening behavior of the oscillator as shown in eq. [3]:

$$k_{\text{eq}} = k_L \left(1 + \frac{3}{4}\alpha Y^2\right) \quad \omega_n = \left(\frac{k_L}{m} \left(1 + \frac{3}{4}\alpha Y^2\right)\right)^{1/2} \quad [3]$$

Figure 2 shows the influence of damping on the amplitude response. The higher the damping the lower is the jump-down frequency and the displacement amplitude. The maximum amplitude and the jump-down frequency are given in eq. [4] (Brennan et al. 2008).

$$Y_d \approx \left(\frac{2}{3\alpha} \left(\left(1 + \frac{3\alpha}{4(\zeta_E + \zeta_M)^2}\right)^{1/2} - 1\right)\right)^{1/2} \quad [4]$$

$$\Omega_d \approx \frac{1}{2^{1/2}} \left(1 + \left(1 + \frac{3\alpha}{4(\zeta_E + \zeta_M)^2}\right)^{1/2}\right)^{1/2}$$

The linear electric dashpot represents the amount of damping injected in the system by the piezoelectric material, thus the power generation is given by the power dissipated by the dashpot.

As shown in Figure 3, the power generation increases until the system jumps down, before which the power reaches the maximum. Moreover, the amount of power that can be extracted depends on the electrical damping injected in the system. When the electrical damping is zero, no power can be harvested, while when the damping is too high, the oscillator does not move and no power is then produced. An optimal electrical damping which maximizes the power generation lies in between. Providing the power spectrums for varying electrical

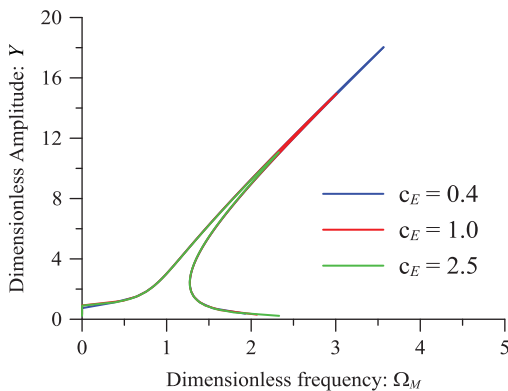


Figure 2 FRF of the Duffing oscillator for different values of electrical damping ($\alpha = 0.048$, $\zeta_M = 0.0056$, $\omega_n = 0.0016$)

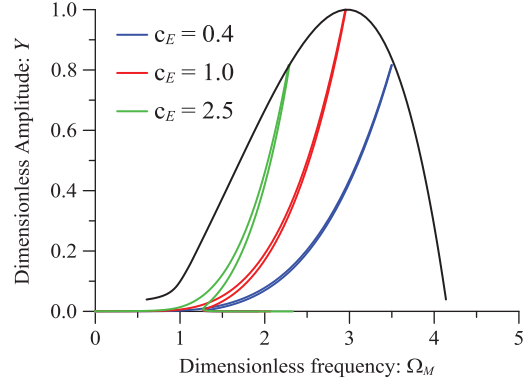


Figure 3 Power response of the Classical Duffing Oscillator for different values of electrical damping

damping, the envelope of all peaks is obtained (black line in Figure 3).

By comparing Figure 3 to the well-known power response of a linear harvester (Du Toit 2005), it is proved that nonlinear harvesters have a much larger bandwidth than linear harvesters which are useful only when operating near the resonance frequency of the system. Computing the power at the jump-down using eq. [4], a closed expression of the maximum power is provided:

$$P_d = \frac{1}{2} C_E |\dot{w}|^2 = \frac{\zeta_E m |\dot{y}_{\text{ext}}|^2}{4\omega_0 (\zeta_M + \zeta_E)^2} \quad [5]$$

Eq. [5] is the same to the result that was obtained for linear harvesters (Roundy 2003), and the peak power occurs when $\zeta_E = \zeta_M$, as it can be shown in Figure 3 or by providing the derivative. The previous expression can be considered as a theoretical upper bound to the power generation for all kind of resonant energy harvesters. However, this does not mean that $\zeta_E = \zeta_M$ is always the optimal condition for the oscillator. However, this is true only at $\Omega = \Omega_d$ (as in linear system it is true only at resonance) while for other excitation frequencies, the optimal electrical damping is higher (when $\Omega < \Omega_d$) or lower (when $\Omega > \Omega_d$) than the mechanical damping. In conclusion, each excitation frequency requires a specific electrical damping for the harvester to work in the optimal condition.

The simple model suggests that the electrical damping needs to match the mechanical damping at the maximum power; thereby eq. [5] provides an upper limit for both linear and nonlinear resonant harvesters. However, the model relies on a strong hypothesis on the piezoelectric coupling, which should take into account the nonlinear behavior. This issue is considered in the following section with more accurate modeling of the piezoelectric coupling.

Accurate model

A more accurate model needs to be developed since the model presented in Section 2 is not suitable to describe the completely coupled piezoelectric behavior. Indeed, a linear dashpot is not sufficient enough to describe the coupling as it was extensively demonstrated (Roundy 2003; Du Toit 2005). For instance, the previous simple model is not able to explain the increase of stiffness due to the piezoelectric coupling. A coupled nonlinear model of a doubly clamped piezo-laminated beam is developed in this paper. The sectional behavior of the beam is studied by means of Classical Lamination Theory (CLT) specifically modified to introduce the piezoelectric coupling and nonlinear strain. By appropriate hypothesizing on the deflection and electric field, a lumped system is obtained and then solved through HBM. The influence of the external load resistance is then studied and the results obtained in Section 2 are confirmed.

Geometry

The doubly clamped beam resonator is presented in Figure 4. L and h are the half length and the total thickness of the piezolaminated beam, respectively. A concentrated mass (m_c) is placed in the middle of the beam. The x_1 -coordinate originates in the neutral axis and is directed downward while x_3 -coordinate lies along the beam axis. A PZT layer is placed on top of the beam substrate and is activated in d33-mode when the beam deflects. To implement d33-mode, interdigitated (IDT) electrodes span one surface of PZT thin film, which has been polarized along x_3 -axis, wraps from one electrode to the next in alternating directions. In such way, when the PZT layer is stretched an electric field arises parallel to the x_3 -axis, the generated charge can be collected by the IDT electrodes. The IDT electrodes are alternatively connected, resulting in a couple of electrodes. One of them is grounded while the other is attached to an external load resistor (R), which represents an ideal external circuit employed for managing the power generated by PZT.

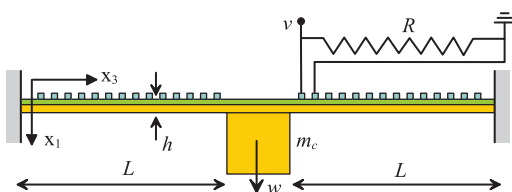


Figure 4 Doubly clamped bridge-shaped piezolaminated beam with tip mass

Sectional behavior: Modified Classical Lamination Theory (MCLT)

The beam's final stack is not homogeneous since different layers are deposited. The mechanical response of the layered beam can be obtained by means of a number of theories (Ballhause et al. 2005). A very thin beam must be designed to activate nonlinear stretching. Thus, CLT is adopted here in order to introduce the piezoelectric coupling in PZT layer and the Green-Lagrange nonlinear strain tensor. The bending (S_{33-L}) and stretching (S_{33-N}) strains along the beam axis are computed from Euler-Bernoulli kinematics assumptions and the Green-Lagrange strain-displacement relationship:

$$S_{33-L} = -x_1 \frac{\partial^2 w_1}{\partial x_3^2} \quad S_{33-N} = \frac{1}{2} \left(\frac{\partial w_1}{\partial x_3} \right)^2 \quad [6]$$

where w_1 and w_3 are the vertical and horizontal displacement of the beam neutral axis.

The electric potential (ϕ) is constant across the piezoelectric layer. Piezoelectric constitutive laws are adopted to describe strain-stress relation, the fully coupled law for d33-mode reads as follows:

$$T_{33} = C_{33}S_{33} - e_{33}E_3 + T_{33}^r \quad D_3 = e_{33}S_{33} + \epsilon_{33}^S E_3 \quad [7]$$

where T_{33} is the stress component parallel to x_3 -axis, T_{33}^r is the residual stress component, S_{33} is the strain tensor component, D_3 the electric displacement component, E_3 the electric field component ($E_3 = -\nabla\phi$) and C_{33} , e_{33} and ϵ_{33}^S are the elastic, piezoelectric and dielectric constant, respectively. Eq. [7] is known as the *e-form* of piezoelectric constitutive relations.

By considering a layered section and by integrating on the thickness, one obtains the generalized stiffness usually defined for the theory of laminates. In such a case, the new constitutive law contains, in the integrated constitutive equations, the generalized stiffness due to residual stresses and the generalized piezoelectric coefficient. Moreover, the same procedure is adopted on the electrical part of the constitutive law obtaining the internal capacity. The same method is applied to compute the equivalent translational and rotational mass of the beam which are summed to the concentrated mass (Ardito et al. 2013).

Lumped model: Rayleigh-Ritz method

Rayleigh-Ritz method is adopted to describe beam deflection and electric potential along the beam. The vertical displacement is modeled as a cubic polynomial

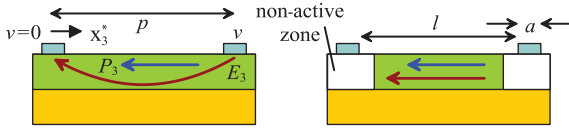


Figure 5 Polarization and electric potential between IDT electrodes

while the electric potential can be considered as linear because the strain is constant between two electrodes (Figure 5). The coordinate x_3^* starts in the middle of each electrode and is directed opposite to the polarization vector P_3 which wraps from one electrode to the next in alternating directions.

$$\begin{aligned} w_1(x_3; t) &= w(t)\psi_w(x_3) = w(t)\left(3(x_3/L)^2 - 2(x_3/L)^3\right) \\ \phi(x_3; t) &= v(t)\psi_v(x_3) = v(t)(x_3^* - a/2)/l \end{aligned} \quad [8]$$

Motion equation

Euler–Lagrange equations are used to compute the motion equation:

$$\frac{d}{dt} \left(\frac{\partial \mathcal{L}}{\partial \dot{q}_i} \right) - \frac{\partial \mathcal{L}}{\partial q_i} + \frac{\partial \mathcal{D}}{\partial \dot{q}_i} = 0 \quad [9]$$

where the Lagrangian is a combination of kinetic energy (\mathcal{K}), internal energy (\mathcal{E}) and external work (\mathcal{W}):

$$\mathcal{L} = \mathcal{K} - (\mathcal{E} - \mathcal{W}) \quad [10]$$

The involved quantities are computed as follows:

$$\mathcal{E} = \frac{1}{2} \int_V T_{33} S_{33} - D_3 E_3 dV = \frac{1}{2} 2 \int_0^L \int_A (T_{33} S_{33} - D_3 E_3) dA dx_3 \quad [11]$$

$$\begin{aligned} \mathcal{K} &= \frac{1}{2} m_{\text{tip}} (\dot{w} + \dot{y}_{\text{ext}})^2 + \frac{1}{2} \int_V \rho (\dot{w}_1 + \dot{y}_{\text{ext}})^2 dV \\ &= \frac{1}{2} m_{\text{tip}} (\dot{w} + \dot{y}_{\text{ext}})^2 + \frac{1}{2} 2 \int_0^L \int_A \rho (\dot{w}_1 + \dot{y}_{\text{ext}})^2 dA dx_3 \end{aligned} \quad [12]$$

$$\mathcal{W} = -qv \quad [13]$$

$$\mathcal{D} = \frac{1}{2} c_M \dot{w}^2 \quad [14]$$

where V and A are the volume of the beam and the area of the beam cross section.

By employing assumptions of eqs [6]–[8], and solving eq. [9] for $q_i = w, v$ the motion equations of the coupled system connected to an external load resistance read:

$$\begin{aligned} m_w \ddot{w} + c_M \dot{w} + (k_l + k_r)w + k_N w^3 - \Theta_{\chi v} v + \Theta_{\eta v} w v &= -m_y \ddot{y}_{\text{ext}} \\ k_E v + \Theta_{\chi v} w - 1/2 \Theta_{\eta v} w^2 &= q \\ \dot{q} &= -R^{-1} v \end{aligned} \quad [15]$$

where m_w is the total mass, m_y is the mass activated by the external acceleration; k_l , k_r and k_N are the linear elastic, the residual stress and the nonlinear stiffness; k_E is the internal capacitance of PZT, $\Theta_{\chi v}$ and $\Theta_{\eta v}$ are the linear and nonlinear coupling coefficients, c_M is the mechanical damping coefficient, and R is the external load resistance. The coefficients are computed by integrating the shape functions and the generalized constitutive coefficients on the volume of the beam.

$$\begin{aligned} \mathcal{E}_{NN} &= \frac{1}{2} \int_V (C_{33} S_{33-N})(S_{33-N}) dV \\ &= \frac{1}{2} \int_V C_{33} \left(\frac{1}{2} \psi'_w{}^2 w^2 \right) dV = \frac{1}{4} k_N w^4 \end{aligned} \quad [16a]$$

$$\begin{aligned} \mathcal{E}_{EL} &= \frac{1}{2} \int_V 2(-e_3 E_3)(S_{33-L}) dV \\ &= \frac{1}{2} \int_V 2(e_3 \psi'_v v)(-x_1 \psi''_w w) dV = -\Theta_{\eta v} v w \end{aligned} \quad [16b]$$

$$\begin{aligned} \mathcal{E}_{EN} &= \frac{1}{2} \int_V 2(-e_3 E_3)(S_{33-N}) dV \\ &= \frac{1}{2} \int_V 2(e_3 \psi'_v v) \left(\frac{1}{2} \psi'_w{}^2 w^2 \right) dV = \frac{1}{2} \Theta_{\eta v} v w^2 \end{aligned} \quad [16c]$$

$$\begin{aligned} \mathcal{E}_{EE} &= -\frac{1}{2} \int_V 2(\varepsilon_3 E_3)(E_3) dV \\ &= -\frac{1}{2} \int_V 2(-\varepsilon_3 \psi'_v v)(-\psi'_v v) dV = -\frac{1}{2} k_E v^2 \end{aligned} \quad [16d]$$

The other coefficients are computed in the same way but they are not reported since they are customary in CLT (Ardito et al. 2013).

Eq. [15] describes the dynamic behavior of the nonlinear harvester. Additional coupling terms arise with respect to a linear harvester. When substituting the aforementioned assumptions in the internal energy expression

(eq. [11]), the nonlinear strain ($\propto w^2$) multiplies the piezoelectric strain ($\propto v$) and an additional “nonlinear coupled term” (eq. [16c]) is obtained. Accordingly to eq. [9], by differentiating with respect to w and v , new nonlinear coupling terms proportional to w appear in eq. [15]. These additional coupling terms are negligible at low w , physically the bending strain prevails on the stretching strain and the beam does not activate the nonlinear regime. In this case, eq. [15] reduces to the classical equations of linear harvesters (Du Toit 2005).

Solution: HBM

The oscillator frequency response to harmonic excitations is studied through HBM. Nonlinear systems do not respond to a monoharmonic signal with a monoharmonic at the same frequency but all harmonics are involved in the response (Worden and Tomlinson 2000). The solution provided by HBM is always an approximation, since to appropriately apply the method the trial solution must be an infinite sum of all harmonics. However, according to physic considerations, one or few of harmonics are enough to correctly describe the dynamics. In this case, the amplitude is well described by a single harmonic, while two harmonics are required to get the correct voltage response since stretching mode has twice the frequency of bending one. Moreover, at large amplitudes, the linear response (described by the first harmonic) can be neglected and only the second harmonic survives. Neglecting the linear coupling terms and substituting the trial solutions $w = W \sin(\omega t)$ and $v = V \sin(2\omega t + \Phi_v)$ in eq. [15], the FRF is computed:

$$Y = \left\{ \left[-\Omega_M^2 + 1 + \left(\frac{3}{4}\alpha + \frac{\kappa_{\eta v}^2 \Omega_M^2}{2(4\Omega_M^2 + \Omega_E^2)} \right) Y^2 \right] + i \left[\left(2\zeta_M + \frac{\kappa_{\eta v}^2 \Omega_E}{4(4\Omega_M^2 + \Omega_E^2)} Y^2 \right) \Omega_M \right] \right\}^{-1} \quad [17]$$

where $\Omega_M = \omega/\omega_n$ is the dimensionless excitation frequency, $\Omega_E = 1/Rk_E\omega_n$ is the dimensionless cut-off frequency of the circuit (Rk_E is the time constant of the RC circuit) and $\kappa_{\eta v} = W_0 \Theta_{\eta v}/(k_E k_L)^{1/2}$ is the effective piezoelectric nonlinear coupling coefficient. $\kappa_{\eta v}$ is a global measure of the degree of coupling which takes into account d33-mode piezoelectric coupling coefficient $\kappa_{33} = e_{33}/(C_{33}\epsilon_{33}^S)^{1/2}$, geometrical and nonlinear aspects. In case of a pure linear piezoelectric system, $\kappa_{\eta v}$ would exactly coincide with κ_{33} .

The equivalent stiffness and damping coefficients depend on the amplitude because of the nonlinear behavior of the system:

$$k_{eq} = k_L \left(1 + \left(\frac{3}{4}\alpha + \frac{\kappa_{\eta v}^2 \Omega_M^2}{2(4\Omega_M^2 + \Omega_E^2)} \right) Y^2 \right) \quad [18]$$

$$\zeta_{eq} = \zeta_M + \zeta_E = \zeta_M + \left(\frac{\kappa_{\eta v}^2 \Omega_E}{8(4\Omega_M^2 + \Omega_E^2)} \right) Y^2$$

For small amplitudes, the nonlinear behavior is not activated, and no damping is injected into the system by the coupling activated by the stretching strain. In this case, the bending strain dominates and the FRF in eq. [17] would reduce to one of a linear harvester where equivalent stiffness and damping do not depend on amplitude (duToit 2005).

The displacement response Y is obtained by solving a cubic equation in Ω_M resulting from the module of eq. [17], and the shape of the response is similar to the Duffing oscillator response. As eq. [18] shows, the external load resistor modifies the stiffness and the damping. According to the value of R , the curve is more (or less) distorted, and the value of jump-down frequency is modified too. In short circuit condition (S.C.), $R \rightarrow 0$ ($\Omega_E \rightarrow \infty$), the stiffness reduces to the equivalent stiffness of the classical Duffing oscillator (eq. [3]), while the electrical damping goes to zero and no energy can be harvested. In open circuit condition (O.C.) $R \rightarrow \infty$ ($\Omega_E \rightarrow 0$), the equivalent stiffness is increased while, as expected, the electrical damping still goes to zero and no energy can be harvested. All intermediate conditions depend on the value of R . Starting from O.C. condition, the damping introduced in the system increases as Ω_E increases, until the maximum damping is reached. After this point, increasing Ω_E reduces the electrical damping injected in the system until the S.C. condition is reached. As a result, the jump-down frequency, which depends on the total damping ratio value, decreases as Ω_E increases, until to a minimum value (blue line in Figure 6), and then grows to reach the S.C. condition.

Electrical damping and power generation

The power generation is computed and plotted in Figure 7 by employing the relation shown in eq. [19]:

$$P = \frac{|V|^2}{R} = m\omega_n^3 \Omega_M^2 \left(\frac{\kappa_{\eta v}^2 \Omega_E}{8(4\Omega_M^2 + \Omega_E^2)} \right) W^4 \quad [19]$$

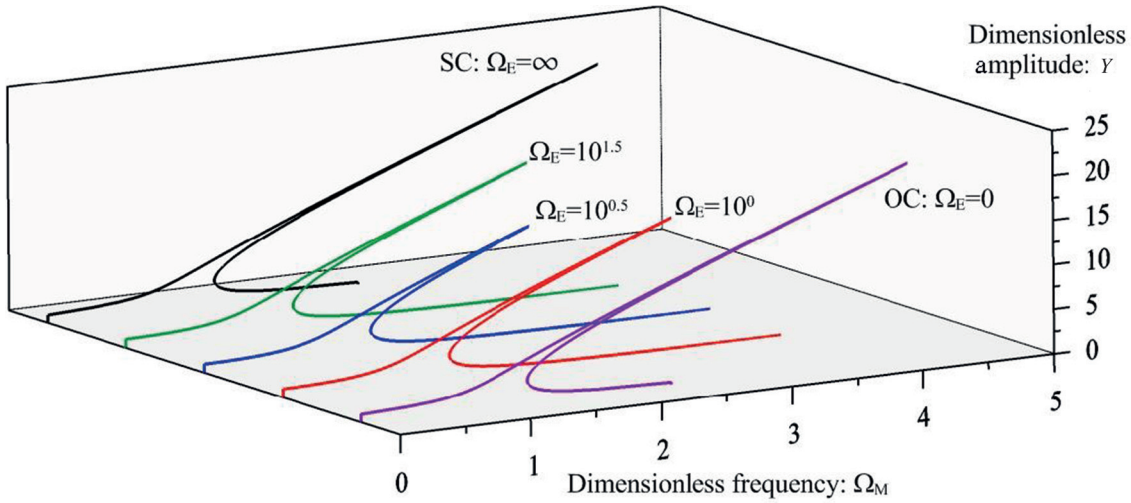


Figure 6 Amplitude response for different values of cut-off frequency

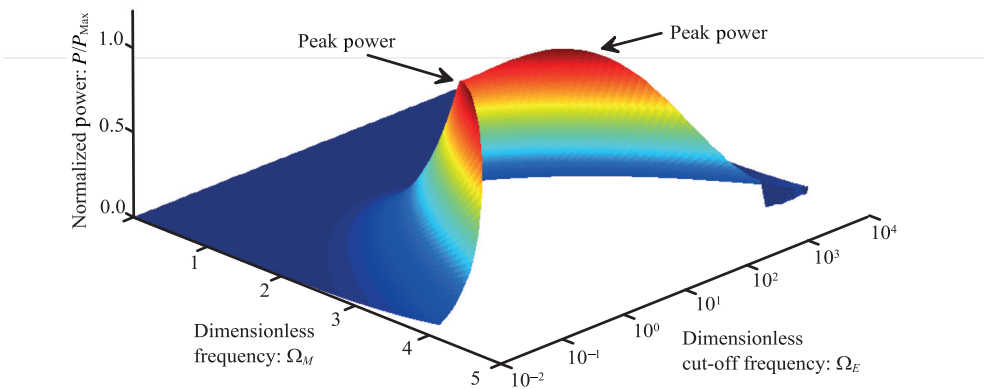


Figure 7 Normalized power generation vs. dimensionless frequency (Ω_M) and cut-off frequency (Ω_E)

The electrical damping injected to the system has a maximum when the displacement amplitude and the jump-down frequency are the lowest. This maximum depends on the value of the effective coupling coefficient $\kappa_{\eta v}$. Two situations must be considered: the peak electrical damping (i) cannot reach or (ii) can overcome the mechanical damping. In the first case, the electrical damping must be pushed to the maximum value in order to maximize the power. However, in this case, the harvester does not work efficiently since the power will always be lower than the maximum allowable for the system. In this second case (Figures 8 and 7), the system results bounded by the mechanical damping, and the power generation has two peaks when $c_E = c_M$. If the electrical damping is pushed

to overcome the mechanical, the total damping injected in the system will excessively reduce the amplitude and lower the power generation.

Conclusion

In this paper, a first theoretical study of a nonlinear piezoelectric harvester is provided. A simple model is developed in which piezoelectric coupling is treated as a linear dashpot added to a nonlinear Duffing oscillator. The main result supports that the power generation is bounded by the mechanical damping for both linear and nonlinear harvesters. However, in the nonlinear

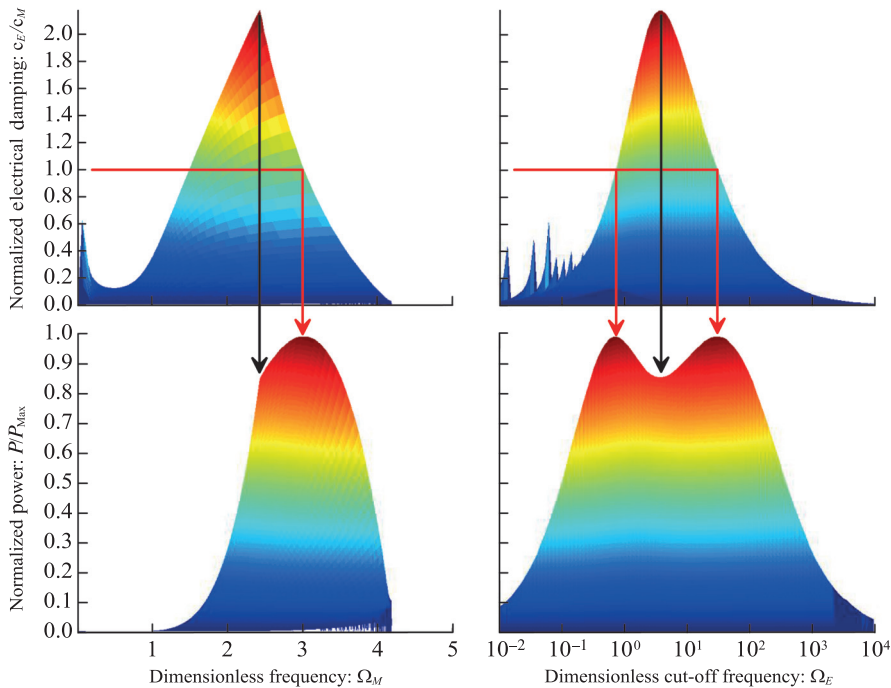


Figure 8 Normalized electrical damping (c_E/c_M upper) and normalized power generation (P/P_{Max} bottom) vs. dimensionless excitation frequency (Ω_M) and dimensionless cut-off frequency (Ω_E). The peak power generation is obtained when $c_E/c_M = 1$

case the power generation is spread out over a wider bandwidth.

A more accurate model is made to study the behavior of a bridge-shaped nonlinear harvester working in d33-mode. The direct influence of an external load resistor is included to consider a more accurate nonlinear coupling effect instead of the linear electrical damping employed in the first model. The sectional behavior of the beam is studied by means of Classical Lamination Theory specifically modified to introduce the piezoelectric coupling and nonlinear Green-Lagrange strain tensor. A lumped model is built through Rayleigh–Ritz method and is solved in the nonlinear regime by means of HBM. By solving the nonlinear FRF, the nonlinear equivalent stiffness and damping can be identified. This second model is suitable for predicting the response of a generic piezoelectric nonlinear harvester with arbitrary excitation frequency and external load.

Acknowledgments: Giacomo Gafforelli thanks Prof. Sang-Gook Kim and the Micro & Nano Systems Laboratory for the opportunity to collaborate and for being hosted as visiting Student at MIT.

Giacomo Gafforelli and Alberto Corigliano thanks Eniac joint undertaking, project Lab4MEMS, grant n° 325622, for partial funding this research.

References

1. Abdelkefi, A., A. H. Nayfeh, and M. R. Hajj. 2012. "Effects of Nonlinear Piezoelectric Coupling on Energy Harvesters under Direct Excitation." *Nonlinear Dynamics* 67(2): 1221–1232.
2. Ardito, R., E. Bertarelli, A. Corigliano, and G. Gafforelli. 2013. "On the Application of Piezolaminated Composites to Diaphragm Micropumps." *Composite Structures* 99:231–240.
3. Ballhause, D., M. D'Ottavio, B. Kröplin, and E. Carrera. 2005. "A Unified Formulation to Assess Multilayered Theories for Piezoelectric Plates." *Computers and Structures* 83(15–16):1217–1235.
4. Brennan, M. J., I. Kovacic, A. Carrella, and T. P. Waters. 2008. "On the Jump-up and Jump-Down Frequencies of the Duffing Oscillator." *Journal of Sound and Vibration* 318(4–5):1250–1261.
5. duToit, N. E. 2005. "Modeling and Design of a Mems Piezoelectric Vibration Energy Harvester." Massachusetts Institute of Technology, Thesis.
6. duToit, N., B. Wardle, and S. G. Kim. 2005. "Design Considerations for Mems-Scale Piezoelectric Mechanical Vibration Energy Harvesters." *Integrated Ferroelectrics* 71:121–160.
7. Hajati, A., and S. G. Kim. 2011. "Ultra Wide Bandwidth Piezoelectric Energy Harvesting." *Applied Physics Letters* 99:083105.
8. Harne, R. L., and K. W. Wang. 2013. "A Review of the Recent Research on Vibration Energy Harvesting via Bistable Systems." *Smart Materials and Structures* 22(2):023001.

9. Jeon, Y. B., R. Sood, J. H. Jeong, and S. G. Kim. 2005. "MEMS Power Generator with Transverse Mode Thin Film PZT." *Sensors and Actuators, A: Physical* 122(1 Spec. Iss):16–22.
10. Kim, S. G., S. Priya, and I. Kanno. 2012. "Piezoelectric MEMS for Energy Harvesting." *MRS Bulletin* 37(11):1039.
11. Roundy, S. 2003. "Energy Scavenging for Wireless Sensor Nodes with a Focus on Vibration to Electricity Conversion." University of California, Thesis
12. Worden, K., and G. R. Tomlinson, eds. 2000. *Nonlinearity in Structural Dynamics: Detection, Identification and Modelling*, 1st ed. London, UK: Institute of Physics Publishing.